Noise-Driven Anisotropic Diffusion Filtering of MRI

Karl Krissian and Santiago Aja-Fernández

***Abstract*—A new filtering method to remove Rician noise from magnetic resonance images is presented. This filter relies on a robust estimation of the standard deviation of the noise and combines local linear minimum mean square error filters and partial differential equations for MRI, as the speckle reducing anisotropic diffusion did for ultrasound images. The parameters of the filter are automatically chosen from the estimated noise. This property improves the convergence rate of the diffusion while preserving contours, leading to more robust and intuitive filtering. The partial derivative equation of the filter is extended to a new matrix diffusion filter which allows a coherent diffusion based on the local structure of the image and on the corresponding oriented local standard deviations. This new filter combines volumetric, planar, and linear components of the local image structure. The numerical scheme is explained and visual and quantitative results on simulated and real data sets are presented. In the experiments, the new filter leads to the best results.**

***Index Terms*—Anisotropic diffusion, LMMSE filter, magnetic resonance imaging, Rician distribution.**

I. Introduction

MAGNETIC resonance imaging (MRI) can be divided into two regimes: relatively high signal-to-noise ratio (SNR) and high resolution with low SNR imaging. There is a tradeoff between SNR, spatial resolution, and acquisition time. Obtaining higher resolution images with a high SNR requires additional acquisition time which is usually limited by parameters such as the patient comfort or by physiological constraints. Efficient methods to reduce the noise are still needed especially in applications requiring a high resolution.

Several filtering methods to improve SNR in MRI have been proposed in literature. The first attempts to estimate the magnitude MR image from a noisy image are that due to Henkelman [1] and the *conventional approach* (CA) proposed by McGibney *et al.* [2]. Sijbers *et al.* [3], [4] estimate the Rician noise level and perform signal reconstruction using a maximum likelihood approach. Expectation-maximization formulations with Rician noise assumptions have been used in SAR imaging [5] and may be also applied in MRI. Wavelet-based methods for noise removal have also been considered, as Nowak's [6]—in which the authors assume an underlying Rician model—or the one due to Pižurica *et al.* [7]. Other techniques involve total variation schemes [8], Partial Differential Equation [9], Markov Random Fields [10] or nonparametric neighborhood statistics techniques like nonlocal means [11], [12] and unbiased NLM [13]–[15] algorithms. Basu *et al.* [16] use a Perona-Malik-like smoothing filter combined with a local Rician data attachment term (effectively trying to remove the intensity bias locally), assuming a known noise level for the Rician noise model. Recently, Koay and Basser in [17] developed a correction scheme to analytically estimate the signal, Martin-Fernandez *et al.* [18] propose an anisotropic Wiener-filter approach and Aja-Fernández *et al.* [19]–[21] proposed a Linear Minimum Mean Square Error (LMMSE) scheme assuming an underlying Rician model.

Alternatively, in ultrasound imaging, Yu and Acton [22] proposed a filter to reduce the speckle, called Speckle Reducing Anisotropic Diffusion or SRAD. This approach combines the standard Perona and Malik anisotropic diffusion (AD) scheme [23] with speckle reducing filters based on the image local statistics [24]. Several extensions and improvements have been studied, among them Aja-Fernández *et al.* [25] showed the importance of an accurate noise estimation and the improvement obtained by using Kuan's filter [26], and Krissian *et al.* [27] extended the filter to a matrix diffusion filter and proposed a semi-implicit numerical scheme which improves its numerical stability.

In this paper, we propose an extension of the SRAD ideas to reduce Rician-distributed noise present in MRI. Since this filter is highly sensitive to the accuracy of the estimated noise standard deviation [25], we use a robust technique to estimate this parameter based on the mode of the local variance of the image intensity. Furthermore, we introduce a new matrix diffusion extension of the scalar partial differential equation (PDE), allowing a better smoothing close to the borders of the different tissues. This extension is more natural than the one introduced in [27] since it takes into account local statistics within neighborhoods of different dimensions: volumetric for the standard scalar diffusion, planar and linear, allowing a better smoothing and preservation of borders and linear structures.

The paper is organized as follows. Section II presents the background in filtering and estimation. Section III presents the new anisotropic filter, in its scalar and matrix form. Results for synthetic and real data are shown in Section IV. Conclusions are presented in Section V.

Manuscript received July 17, 2008; revised May 13, 2009. First published June 19, 2009; current version published September 10, 2009. This work was supported in part by the Comisión Interministerial de Ciencia y Tecnología research grant TEC2007-67073, research grant USIMAG TEC 2004 06647-C03-02; in part by the Fondo de Investigaciones Sanitarias for grant PI-041483; and in part by the Junta de Castilla y León for grant VA026A07. The associate editor coordinating the review of this manuscript and approving it for publication was Dr. Dimitri Van De Ville.

K. Krissian is with the with the Spanish Ministry of Science and Innovation and the Centro de Tecnología Médica, Dep. de Señales y Comunicaciones, Pabellón B, Edificio Telecomunicaciones Lab. 203, Universidad de Las Palmas de Gran Canaria, Campus de Tafira, 35017 Las Palmas, Spain (e-mail: krissian@dis.ulpgc.es).

S. Aja-Fernández is with LPI, ETSI Telecomunicación, Universidad de Valladolid, Spain (e-mail: sanaja@tel.uva.es).

Color versions of one or more of the figures in this paper are available online at http://ieeexplore.ieee.org.

Digital Object Identifier 10.1109/TIP.2009.2025553

II. Background

A. LMMSE Estimator for the Rician Model

Noise in magnitude Magnetic Resonance (MR) images is usually modeled following a Rician distribution, due to the existence of uncorrelated Gaussian noise with zero mean and the same variance σ_n^2 in both the real and imaginary parts of the complex k-space data [28]. In the image background, where the SNR is zero due to the lack of water-proton density in the air, the Rician PDF simplifies to a Rayleigh distribution.

The filtering method proposed in this paper is based on the Linear Minimum Mean Square Error (LMMSE) estimator for the Rician model, proposed in [19] and [20] as

$$\widehat{A^2(\mathbf{x})} = \left\langle M(\mathbf{x})^2 \right\rangle - 2\sigma_n^2 + K(\mathbf{x})\left(M^2(\mathbf{x}) - \left\langle M(\mathbf{x})^2 \right\rangle\right) \quad (1)$$

where $M(\mathbf{x})$ is the magnitude value of the N-dimensional point $\mathbf{x}$ in an MR volume and $A(\mathbf{x})$ is the original signal level if no noise is present. In order to achieve a closed-form expression, A^2 is used instead of A. $K(\mathbf{x})$ is defined as [19]

$$K(\mathbf{x}) = 1 - \frac{4\sigma_n^2\left(\left\langle M(\mathbf{x})^2 \right\rangle - \sigma_n^2\right)}{\left\langle M(\mathbf{x})^4 \right\rangle - \left\langle M(\mathbf{x})^2 \right\rangle^2}. \quad (2)$$

The operator $\langle . \rangle$ denotes the sample estimator of the expectation, that may be defined as

$$\langle M(\mathbf{x}) \rangle = \frac{1}{|\eta(\mathbf{x})|} \sum_{\mathbf{p} \in \eta(\mathbf{x})} M(\mathbf{p}) \quad (3)$$

where $\eta(\mathbf{x})$ is a neighborhood centered at the pixel $\mathbf{x}$ and $|\eta(\mathbf{x})|$ is the size of the neighborhood.

Note that the parameter σ_n^2 must be properly estimated. To this end, many methods has been previously reported. They are mainly based on the features of the Rayleigh background [19], [29]–[31], as, for instance

$$\widehat{\sigma_n} = \sqrt{\frac{2}{\pi}} \operatorname{mode}\left\{\langle M(\mathbf{x}) \rangle\right\}. \quad (4)$$

If the background assumption does not hold, the estimation may be performed using the local variance [19]

$$\widehat{\sigma_n^2} = \operatorname{mode}\left\{\operatorname{Var}\left(M(\mathbf{x})\right)\right\} \quad (5)$$

where $\operatorname{Var}(M(\mathbf{x}))$ is the (unbiased) local sample variance of $M(\mathbf{x})$. Note that this last estimator is defined only to be used in Rician regions of the image.

B. Anisotropic Diffusion Schemes Based on Local Statistics

Based on the pioneer work of Perona and Malik [23], Yu and Acton [22] have proposed a new filter adapted to the statistics of the speckle in Ultrasound images. The main idea behind the SRAD filter is to transform a typical LMMSE estimator of the form

$$\widehat{f(\mathbf{x})} = \langle g(\mathbf{x}) \rangle + K(\mathbf{x})\left(g(\mathbf{x}) - \langle g(\mathbf{x}) \rangle\right) \quad (6)$$

where $\hat{f}$ is an estimator of the original signal f, g is the observed signal, K is a gain function depending on g, and $\langle g \rangle$ is a sample estimator of g; into a Partial Differential Equation (PDE) of the form:

$$\begin{cases} u(\mathbf{x}, 0) = g \\ \frac{\partial u(\mathbf{x},t)}{\partial t} = \operatorname{div}\left(c \nabla u(\mathbf{x}, t)\right) \end{cases} \quad (7)$$

where $c = c(\mathbf{x}, t) = 1 - K(\mathbf{x}, t)$ is a diffusion function depending on the local statistics of the image and on the noise model. More details about the relation between (6) and (7) can be found in [22] and [27].

In the typical Perona and Malik's anisotropic diffusion equation, the diffusion term $c(\mathbf{x}, t)$ is a decreasing function of the gradient norm of the type

$$c(\mathbf{x}, t) = c\left(\|\nabla u(\mathbf{x}, t)\|\right) = e^{-\left(\frac{\|\nabla u(\mathbf{x},t)\|}{\tau}\right)^2}$$

where τ is a free parameter that has to be manually tuned according to intensity gradients generated from both the noise and the relevant contours of the image. Since the image can contain a wide range of magnitudes of relevant intensity gradients, tuning the parameter τ often ends up being a difficult task.

In this last equation, the diffusion is controlled by the local statistics in the image, rather than by an additional chosen parameter. The term $\operatorname{div}(c\nabla u(\mathbf{x}, t))$ in (7) can be rewritten as $c\operatorname{div}(\nabla u(\mathbf{x}, t)) + \nabla c \cdot \nabla u(\mathbf{x}, t)$ to better understand its behavior. In this case, if the observed local standard deviation is characteristic of the noise ($K \to 0$ and $c \to 1$), we are in an homogeneous region and apply the heat equation. If not, K is closer to 1, we reduce the filtering and enhance the contours where c reaches a local minimum.

This approach is attractive because it extends the Perona and Malik filter [23] in a way that obviates the need to choose the main parameter of this filter: the contrast parameter based on the gradient norm. Instead, the amount of diffusion applied in a small neighborhood is based on the local statistics of the image intensity and on the global statistics of the noise which are estimated for the whole image. This filter, the so-called Speckle Reducing Anisotropic Diffusion (SRAD), also converges faster because it tries to remove just the amount of noise contained in the image and this amount is decreasing at each iteration. In [25], an alternative implementation decoupling the estimation and the filtering is done, and in [27], an oriented version of the filter is proposed. We must recall, as it was shown in [25], that the goodness of the filter is totally related with the capability of properly estimate the noise parameter related to the assumed noise model.

III. Rician Noise Driven Anisotropic Diffusion

A. Derivation of the Filter

In this section, we propose an anisotropic diffusion filter for Rician-distributed noise based on the LMMSE filter previously described and the Speckle Reducing Anisotropic Diffusion (SRAD) proposed in [22]. We call it Rician Noise Reducing Anisotropic Diffusion (RNRAD) filter.

If the original signal is defined by $f(\mathbf{x}) = A^2(\mathbf{x}) + 2\sigma_n^2$, the observed signal by $g(\mathbf{x}) = M^2(\mathbf{x})$, then $E\{f(\mathbf{x})\} = E\{g(\mathbf{x})\}$. The LMMSE estimator in (1) may be rewritten in the form of (6) with

$$K(\mathbf{x}) = 1 - \frac{4\sigma_n^2\left(\langle g(\mathbf{x})\rangle - \sigma_n^2\right)}{\mathrm{Var}\left(g(\mathbf{x})\right)}. \tag{8}$$

The corresponding PDE is given by (7), and is applied iteratively using either an explicit or a semi-implicit numerical scheme.

At the end of the diffusion process, the output $u(\mathbf{x}, t)$ is an approximation of the original image $f(\mathbf{x})$. The output image will be

$$\widehat{A}(\mathbf{x}, t) = \sqrt{\max\left(u(\mathbf{x}, t) - 2\sigma_n^2(0), 0\right)} \tag{9}$$

being $\sigma_n(0)$ the σ_n noise parameter in the original image (before filtering).

This proposed scheme has the advantage of not depending on the norm of the gradient for the filtering which can vary in the image, as the AD schemes usually do. In addition, there is a natural decrease of the diffusion as the estimated standard deviation of the noise decreases. This way, computations converge without smoothing out interesting features of the image.

B. Matrix Extension

In [27], a matrix extension to the SRAD filter in the context of ultrasound images is introduced. By combining the approach of Yu and Acton with a matrix anisotropic diffusion, a nonscalar component which can perform directional filtering of the image along the structures is added. This extension to a matrix diffusion takes advantage of the local orientation of the structures in the image to enforce their coherence along directions of minimal intensity change.

In this paper, we propose a new matrix extension of the initial scalar diffusion equation, which takes better into account the statistical properties of the local structure in the image, and improves the overall performance of the filter. As compared to the matrix extension proposed in [27], we propose here a more natural extension.

- The local orientation of the structure is computed based on the structure tensor instead of the local gradient and principal curvature directions. Although the orientation based on the principal curvature directions is a good choice for tubular structures, it has the disadvantage of not being defined at locations where the gradient is null and leads to a less continuous representation.
- Instead of choosing the second and third eigenvalues of the diffusion matrix as the maximal and minimal curvatures, we propose here to relate them to the local statistics of the image in the plane and the line defined by their respective eigenvectors as described later in this section. This choice constitutes a more natural extension of the scalar diffusion to a matrix diffusion and can be easily generalized and applied to a space of any dimension, the 1-D case being equal to the original scalar diffusion equation.

1) Description of the Local Structure: As mention in previous works, (7) can written as $\partial u(\mathbf{x}, t)/\partial t = \mathrm{div}(D\nabla u(\mathbf{x}, t))$, where the diffusion matrix $D = (1 - K(\mathbf{x}, t))I_d$ is a scalar, and I_d denotes the identity matrix. The eigenvectors of the diffusion matrix can be chosen to describe the local structure or geometry of the image. From the different techniques to compute them (see comparisons in [32]–[35]), we will choose the structure tensor [36], for having the advantage of being able to extract the directions of minimal intensity change even in the case of low or zero gradients (for example at the center of linear structures or between two structures of the same intensities).

To describe the structure tensor, different techniques have been developed. For the sake of simplicity we will use the outer product of the gradient, smoothed by a Gaussian convolution [37]

$$T_{\sigma_1,\sigma_2}(u) = G_{\sigma_2} * \left(\nabla_{\sigma_1} u . \nabla_{\sigma_2} u^t\right) \tag{10}$$

where G_{σ_2} is a Gaussian kernel of standard deviation σ_2, $\nabla_{\sigma_1} u$ is the gradient of the image u obtained by convolution with the derivatives of a Gaussian kernel of standard deviation σ_1. Let us denote $\mu_1 \geq \mu_2 \geq \mu_3 \geq 0$ its eigenvalues and $\mathbf{e}_1, \mathbf{e}_2, \mathbf{e}_3$ its associated eigenvectors. $\mathbf{e}_1$ gives the local orientation of maximal intensity variation (which is the gradient orientation in the limit case $\sigma_2 = 0$), and $\mathbf{e}_3$ gives the local orientation of minimal intensity variation.

2) New Matrix Formulation: To naturally extend the RNRAD filter to a matrix diffusion, we design a diffusion matrix D that shares the eigenvectors $\mathbf{e}_i$, $i \in [1, N]$ of T_{σ_1}, σ_2 but with eigenvalues $\lambda_1, \lambda_2, \lambda_3$ related to the level of noise and defined as

$$\begin{aligned}
\lambda_1 &= 1 - K \\
\lambda_2 &= 1 - K + \frac{3}{2}(1 - K_p) \\
\lambda_3 &= 1 - K + \frac{3}{2}(1 - K_p) + 3(1 - K_l)
\end{aligned} \tag{11}$$

where $K = K(\langle u\rangle, \mathrm{Var}(u))$ as defined in (8) is the gain coefficient in a local isotropic neighborhood, $K_p = K(\langle u\rangle_{\mathbf{e}_2,\mathbf{e}_3}, \mathrm{Var}(u)_{\mathbf{e}_2,\mathbf{e}_3})$ is the gain in a local planar neighborhood defined by the eigenvectors $\mathbf{e}_2$ and $\mathbf{e}_3$, and $K_l = K(\langle u\rangle_{\mathbf{e}_3}, \mathrm{Var}(u)_{\mathbf{e}_3})$ is the gain in a local linear neighborhood oriented by the eigenvector $\mathbf{e_3}$. The local mean values are computed as follows, at a voxel position $\mathbf{x}$

$$\langle u\rangle_{\mathbf{e}_2,\mathbf{e}_3} = \frac{1}{25}\sum_{i,j=-2,-2}^{2,2} u(\mathbf{x} + i\mathbf{e}_2 + j\mathbf{e}_3) \tag{12}$$

$$\langle u\rangle_{\mathbf{e}_3} = \frac{1}{7}\sum_{i=-3}^{3} u(\mathbf{x} + i\mathbf{e}_3) \tag{13}$$

and the local variances are computed using the same sets of neighborhoods. In all our experiments, we have set the local isotropic, planar and linear neighborhoods to the following respective sizes: $3 \times 3 \times 3$, 5×5, and 7.

Because the difference between the local mean of a voxel and its intensity can be approximated in 3-D, 2-D, and 1-D, respectively by 1/6, 1/4, and 1/2 of the local Laplacian operator, we

weighted in (11) each type of diffusion by the corresponding coefficient, multiplied by 6 to be homogeneous with the scalar case that uses $1-K$ as diffusion function. In the basis $(\mathbf{e}_1, \mathbf{e}_2, \mathbf{e}_3)$, the diffusion matrix D is diagonal and can be written as

$$D = \begin{bmatrix} \lambda_1 & 0 & 0 \\ 0 & \lambda_2 & 0 \\ 0 & 0 & \lambda_3 \end{bmatrix}. \tag{14}$$

The corresponding diffusion equation can be written as the sum of three diffusion terms

$$\begin{aligned} \frac{\partial u(\mathbf{x},t)}{\partial t} &= \operatorname{div}(D\nabla u) \\ &= 6\left[\frac{1}{6}\operatorname{div}\left((1-K)\nabla u\right) + \frac{1}{4}\operatorname{div}\left((1-K_p)\nabla_p u\right)\right. \\ &\quad \left. + \frac{1}{2}\operatorname{div}\left((1-K_l)\nabla_l u\right)\right] \end{aligned} \tag{15}$$

where $\nabla_p u$ is the projection of the gradient in the plane formed by (e_2, e_3) and $\nabla_l u$ is the projection of the gradient in the direction of e_3. The advantage of this approach is that all the directions will benefit from a progressive filtering which tries to smooth the image just the amount needed to reduce the estimated level of noise. Also, it takes into account the fact that all directions should not be treated equivalently when close to a contour, and in the hypothetical case of a straight circular cylinder, the filtering applied in the direction of the axis of the cylinder would be the same as in a homogeneous noisy region, while the filtering across the boundary will be reduced, leading to potential enhancement in this direction. Fig. 1 illustrates the effect of our filter on a synthetic noisy image representing a cube. The proposed filter is the sum of a scalar, a planar and a linear filter, each of them oriented in the local directions of less intensity variation.

C. Numerical scheme

We denote $c(\mathbf{x},t) = 1 - K(\mathbf{x},t)$ the diffusion coefficient at time t. The PDE can be discretized using an explicit scheme

$$\begin{aligned} u^{k+1}(\mathbf{x}) &= u^k(\mathbf{x}) + dt\operatorname{div}(c\nabla u) \\ &= u^k(\mathbf{x}) + dt\sum_{\mathbf{n}\in\eta} c^k_{\mathbf{n}}\left(u^k(\mathbf{n}) - u^k(\mathbf{x})\right) \end{aligned} \tag{16}$$

where η is the neighborhood of the point $\mathbf{x}$ consisting in the direct neighbors in each direction (typically 4 neighbors in 2-D and 6 in 3-D, but diagonal neighbors could be added as proposed in [9]), $c^k_{\mathbf{n}}(\mathbf{x}) = (c^k(\mathbf{n}) + c^k(\mathbf{x}))/2$ is the mean value of the diffusion coefficient between the position $\mathbf{x}$ and its neighbor pixel $\mathbf{n}$. As in [27], we use a multithreaded version of Jacobi numerical scheme to solve the diffusion PDE. This scheme applied to (16) is written as

$$u^{k+1}(\mathbf{x}) = \frac{u^k(\mathbf{x}) + dt\sum_{\mathbf{n}\in\eta} c^k_{\mathbf{n}} u^k(\mathbf{n})}{1 + dt\sum_{\mathbf{n}\in\eta} c^k_{\mathbf{n}}}. \tag{17}$$

In practice, it is stable for any time step dt and the processing time of one iteration is comparable to the explicit scheme, with a much better convergence rate.

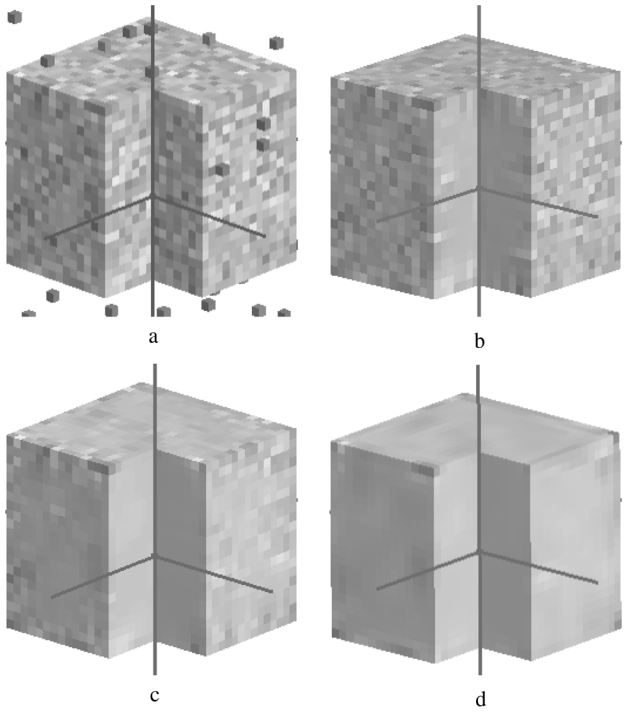

Fig. 1. Illustration of the effect of combining scalar, planar, and linear filtering on a noisy synthetic image of a cube object. The voxels of intensity higher than a threshold are rendered in 3-D, and the cube is cut at the position of the cursor to see its interior. (a) Initial noisy image, (b) scalar filter, (c) scalar + planar combination, (d) scalar + planar + linear combination.

The parallel between (6) and (7), based on $\langle g\rangle - g \approx (1/|\eta|)\operatorname{div}(g)$ suggests using of the value $dt = 1/|\eta|$ as a constant time step. In our case for 3-D images, we set $dt = 1/6$. We refer the reader to a previous work [32] for the discretization of the matrix diffusion equation.

D. Estimation of the Parameters

The proposed filter will remove the noise in the square intensity image by evolving (7) with the parameter $K(\mathbf{x},t)$. Estimates of the parameter $\sigma_n^2(t)$ and also of the local mean and standard deviation are, therefore, needed.

1) Estimation of σ_n^2: Parameter $c(\mathbf{x},t)$ is time dependent in the proposed scheme, and accordingly so will be $\sigma_n = \sigma_n(t)$. If a discrete numerical scheme is assumed, a value for each iteration is considered, i.e. $\sigma_n[k]$. Note that this value must be then estimated in each iteration. We must assume that the Rician model holds once the image is filtered. In [20], it is shown that for a recursive LMMSE filter the assumption is not far from reality. There is a slight mismatch with increasing numbers of iterations, but the Rician assumption is still reasonable. Furthermore, when the SNR gets smaller, the Rician and Gaussian distribution converges as expected for high SNR values.

Most of the noise estimators for MR are based on the assumption of a background where there is no signal, and, therefore, the data follows a Rayleigh distribution. This could be the case for the image before filtering. However, once the diffusion process has began, the volume we are considering, say $u(\mathbf{x})$, is biased with respect to the original image $A(\mathbf{x})$. So, any estimation based on noncentral statistics will also be biased.

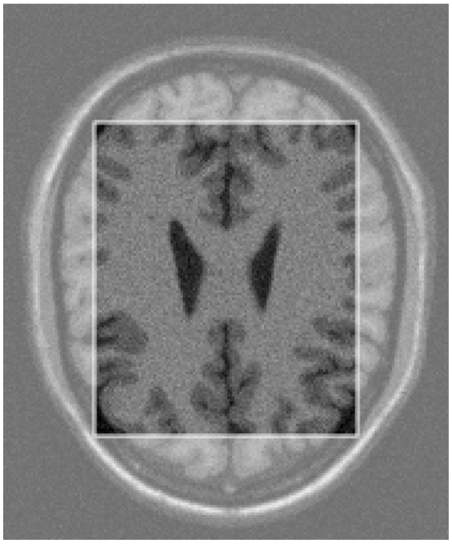

Fig. 2. Region selection for noise estimation. The selected area should be inside the tissue part of the MR, and no background should be considered. It is not required for the area to be uniform.

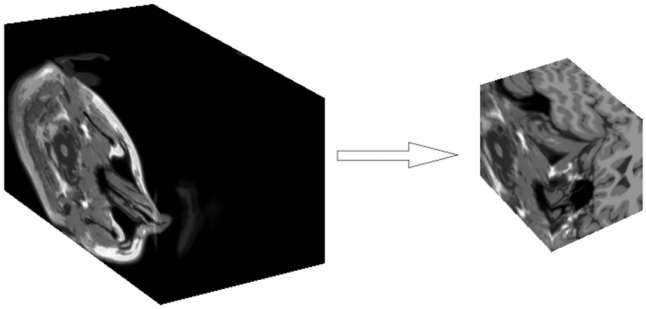

Fig. 3. Three-dimensional region selection for noise estimation. From the $181 \times 217 \times 181$ original volume a $100 \times 90 \times 100$ volume is selected.

From the available methods to estimate the noise from magnitude MR data, we have selected the one in (18); the estimation is done using the variance in a subvolume $\mathbf{x_R}$ inside the skull where there are more tissue regions than background, and, therefore, the Rician assumption holds. The estimator will be

$$\widehat{\sigma_n}^2[k] = \text{mode}\left\{\text{Var}\left(\sqrt{u^k(\mathbf{x_R})}\right)\right\} \tag{18}$$

being $u^k(\mathbf{x_R})$ a segmented region of the volume inside the head, i.e., a region with signal and no background $\mathbf{x_R}$. This region may be roughly defined, as shown (for one slice) in Fig. 2, and (for the whole volume) in Fig. 3. This way, we are assuring that the background has no effect over the estimation. Another rough automatic segmentation method on an inner area may be used; using for instance some thresholding method, as the ones proposed in [38] and [39].

The election of this estimator is two-folded: 1) the variance it is not a central moment, and, therefore, it is not affected by the bias during the process; and 2) according to [40], this estimation is similar to the estimation of the variance of additive Gaussian noise in images. Thus, although the Rician assumption does not hold after several iterations, we can always approximate the noise as additive Gaussian. So, if we assume that the noise distribution tends to Gaussian after the first diffusion steps, the same noise estimator will still be valid through all the iterative process. However, one could use an alternative estimator from those proposed in literature.

2) Estimation of the Image Local Statistics: The local mean $\langle g(\mathbf{x})\rangle$ and the local variance $\text{Var}(g(\mathbf{x}))$ of the observed signal $g(\mathbf{x})$ are computed within a small vicinity of the current position $\mathbf{x}$. In a recent study [25], local statistics in 2-D are computed using a larger neighborhood than the 4 direct neighbors used by Yu and Acton, leading to better results and better stability. This is justified in ultrasound images which are degraded by a stronger noise.

IV. Experiments

A. Synthetic Experiments

To compare the experimental results to a ground truth, synthetic images containing different levels of noise are considered. Our method is quantitatively evaluated on a simulated structural MR data. The structural MR volume contains 256 gray levels, has a size of $181 \times 217 \times 181$ voxels, and is originally noise-free. It has been obtained from the BrainWeb database [41]. We corrupt the data with synthetic Rician noise of different σ_n values.

The noisy volume is processed using the following techniques and parameters.

1) The *Conventional Approach*, denoted CA, by McGibney *et al.* [2], using $3 \times 3 \times 3$ windows and manually setting the exact value of σ_n.
2) The *Analytically Exact Solution*, proposed by Koay and Basser in [17], denoted Koay, using $3 \times 3 \times 3$ windows for statistics computation.
3) The *wavelet domain noise filter* for medical imaging proposed by Pižurica *et al.* in [7]. The best results for this experiment are achieved using $K = 5$.
4) The *LMMSE Estimator* for Rician Noise proposed by Aja-Fernández *et al.* [20], using $3 \times 3 \times 3$ windows both for filtering and noise estimation. The noise estimation is performed using (4).
5) A *Recursive LMMSE Estimator* (RLMMSE) as proposed in [20] with 8 iteration steps, using $3 \times 3 \times 3$ windows both for filtering and noise estimation. Noise estimation done using (4).
6) *Anisotropic Diffusion* of Perona and Malik, denoted AD, where the we use Green's diffusion function defined as $c(\|\nabla u\|) = \tanh(\|\nabla u\|/\tau)/\tau\|\nabla u\|$, with a contrast parameter based on the gradient norm of $\tau = 5$, and 30 iterations with a time-step of 0.1.
7) The *Nonlocal means* algorithm [42], denoted NLM. Recently, a fast version of the algorithm has been proposed in the context of 3-D medical images [12], we use here a similar implementation (see [15]) which allows filtering the whole volume in a reasonable time, with a searching window size of 9^3, and a value of the parameter h that weights the pattern similarity values of 8, we refer to [12] for a discussion about how to choose this parameter.
8) An *Unbiased Nonlocal means* algorithm as proposed in [15], denoted NLCA, for Nonlocal means Conventional

TABLE I
QUALITY MEASURES: SSIM, QILV, AND MSE FOR THE 3-D VOLUME EXPERIMENTS. THE BEST VALUE OF EACH COLUMN IS HIGHLIGHTED. THE PROPOSED SCHEMES (RNRAD) SHOW BETTER RESULTS IN TERMS OF NOISE REMOVAL AND EDGE PRESERVATION

	$\sigma_n = 5$			$\sigma_n = 7$			$\sigma_n = 10$		
	SSIM	QILV	MSE	SSIM	QILV	MSE	SSIM	QILV	MSE
Noise	0.9298	0.9955	26.49	0.8744	0.9868	52.9937	0.7867	0.9579	110.17
AD	0.9202	0.8257	72.60	0.9098	0.8221	77.05	0.8937	0.8164	87.18
Wavelet	0.8996	0.9844	53.60	0.8816	0.9837	65.51	0.8539	0.9783	87.07
NLM	0.9641	0.9565	26.37	0.9533	0.9539	30.27	0.9347	0.9482	40.21
Koay	0.9308	0.6963	81.91	0.9185	0.6920	89.19	0.8986	0.6839	106.31
CA	0.9417	0.7062	69.75	0.9382	0.7079	70.87	0.9310	0.7117	73.40
NLCA	0.9721	0.9576	23.02	0.9709	0.9577	23.67	0.9678	0.9573	25.30
LMMSE	0.9732	0.9980	14.78	0.9552	0.9962	25.26	0.9263	0.9925	42.48
RLMMSE	0.9781	0.9980	13.87	0.9668	0.9959	22.87	0.9515	0.9912	36.68
SRNRAD	0.9808	0.9979	12.49	0.9719	0.9961	19.78	0.9599	**0.9928**	30.35
ORNRAD	**0.9887**	**0.9982**	**7.58**	**0.9836**	**0.9964**	**11.26**	**0.9756**	0.9924	**16.84**

	$\sigma_n = 15$			$\sigma_n = 20$			$\sigma_n = 25$		
	SSIM	QILV	MSE	SSIM	QILV	MSE	SSIM	QILV	MSE
Noise	0.6567	0.8565	252.25	0.5565	0.7053	452.33	0.4812	0.5432	710.62
AD	0.8707	0.8087	115.30	0.8520	0.8041	160.86	0.8327	0.8051	229.59
Wavelet	0.8104	0.9680	124.44	0.7770	0.9469	166.67	0.7513	0.9202	214.50
NLM	0.9051	0.9365	68.98	0.8792	0.9210	115.87	0.8550	0.9029	184.62
Koay	0.8679	0.6673	153.81	0.8412	0.6483	228.84	0.8165	0.6276	336.86
CA	0.9139	0.7197	80.21	0.8924	0.7311	90.54	0.8676	0.7436	104.99
NLCA	0.9576	0.9577	29.86	0.9379	0.9581	**38.11**	0.9071	0.9586	52.16
LMMSE	0.8789	0.9841	72.40	0.8343	0.9731	104.33	0.7924	0.9590	140.16
RLMMSE	0.9303	0.9774	58.45	0.9118	0.9572	78.70	0.8961	0.9294	98.50
SRNRAD	0.9410	**0.9859**	46.83	0.9242	**0.9777**	61.40	0.9075	**0.9677**	75.96
ORNRAD	**0.9603**	0.9824	**26.96**	**0.9432**	0.9692	38.61	**0.9251**	0.9536	**51.90**

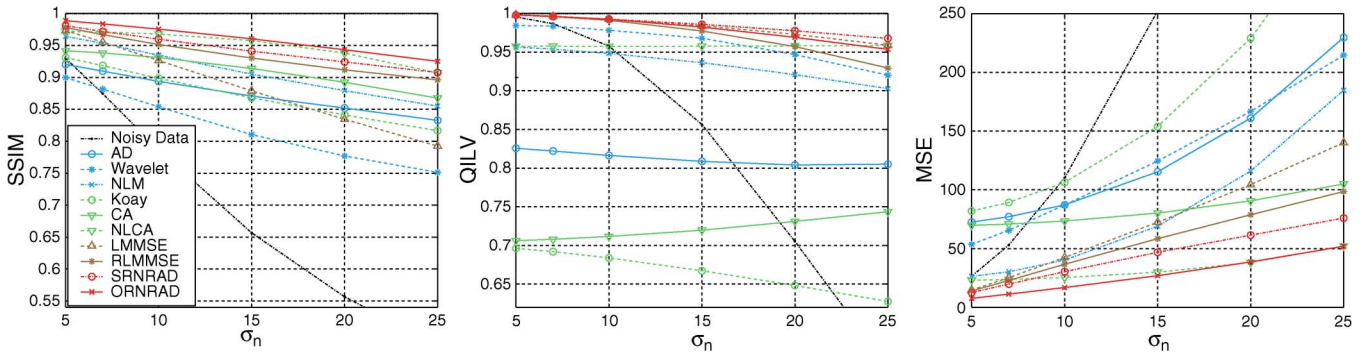

Fig. 4. Quality measures: SSIM, QILV, and MSE for the 3-D volume experiments. The proposed scheme (RNRAD) shows better results in terms of noise removal and edge preservation.

Approach [15]. Other versions of unbiased NL-means algorithms have been proposed in [13] and [14]. We have used a searching window size of 9^3 and a parameter h (defined in [15]) of value 8.

9) The proposed *Rician Noise Reducing Anisotropic Diffusion (RNRAD) filter for MRI*, using either the scalar, denoted Scalar-RNRAD or SNRAD, or the matrix version, denoted Oriented-RNRAD or ORNRAD. For both versions, we use a total diffusion time of $T = 2$, a time-step $dt = 1/6$ and a $3 \times 3 \times 3$ neighborhood for estimating the local statistics. For the matrix version, we use Gaussian kernels with $\sigma_1 = 0.7$ and $\sigma_2 = 1.0$ for computing the Structure Tensor.

To compare the restoration performance of the different methods, two quality indexes are used: the Structural Similarity (SSIM) index [43] and the Quality Index based on Local Variance (QILV) [44]. Both give a measure of the structural similarity between the ground truth and the estimated images.

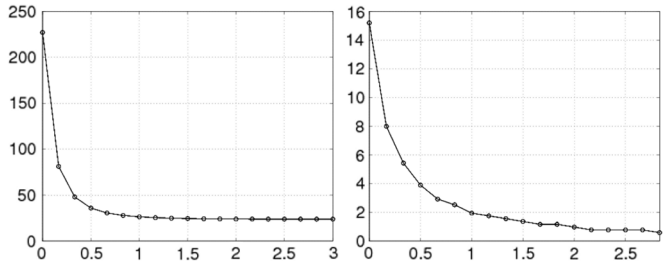

Fig. 5. Evolution of the mean square error (left) and the noise standard deviation estimation (right) as function of the equation diffusion time for $\sigma_n = 15$.

However, the former is more sensitive to the level of noise in the image and the latter to any possible blurring of the edges. Both indexes are bounded; the closer to one, the better the image. The mean square error (MSE) is also calculated. These three quality measures are only being applied to those areas of the original image greater than zero; this way the background

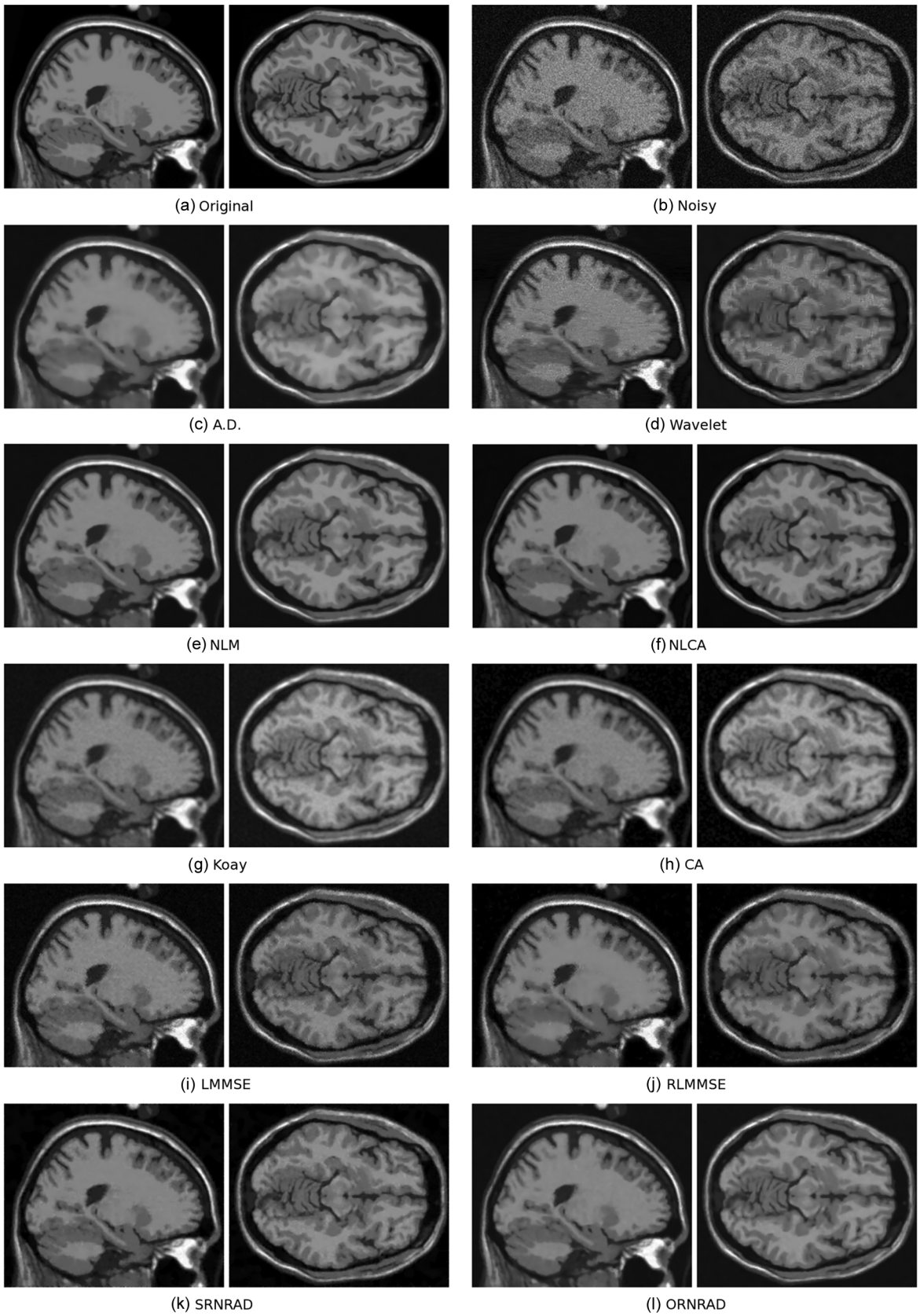

Fig. 6. Results of different denoising filters on a simulated Brain MR volume corrupted with a Rician noise of standard deviation $\sigma_n = 15$. Sagittal (left) and Axial (right) slices. From left to right and top to bottom: (a) the original image, (b) the noise corrupted image, and the results of (c) the anisotropic diffusion filter, (d) the wavelet filter, (e) the nonlocal means filter, (f) the nonlocal conventional approach, (g) the analytically exact solution referred to as Koay and Basser's filter, (h) the Conventional Approach, (i) the LMMSE filter for Rician noise, (j) the Recursive LMMSE filter, (k) the Scalar Rician Noise Reducing Anisotropic Diffusion, and (l) the Oriented Rician Noise Reducing Anisotropic Diffusion.

is not taken into account when evaluating the quality of each method. The average of ten experiments is considered for each σ_n and each filter.

Results are detailed in Table I and Fig. 4, and depicted in Fig. 6 corresponding respectively to sagittal and axial cuts of the volume dataset. Our new algorithm outperforms the other compared techniques for all three quality assessment measures and all levels of noise, apart from one case with a noise standard deviation of 20, where the unbiased nonlocal means algorithm (NLCA) gives a slightly better value for the MSE measure. The matrix version gives better results than the scalar one for both the SSIM and MSE measures, while the scalar version gives slightly better results for the QILV measure with noise standard deviations 10, 15, 20, and 25.

This difference can be explained by the additional smoothing along the edges performed by the matrix version of our algorithm which also introduces a slight blurring. In Table I, we distinguish and separate biased algorithms: anisotropic diffusion, wavelets and nonlocal means, from nonbiased algorithms. Among the biased algorithms, we observe a clear advantage of the NL-means algorithms, which also gives very good visual results in Fig. 6. However, since the bias is not removed, it does not reach as good restoration performance as most bias-free algorithms. Among the unbiased algorithms, the unbiased NL-means algorithms obtain good results in terms of MSE measure as compared to other existing approaches, but still our new filter outperforms it in most cases. One reason for the better results obtained by our filter is that it automatically adapts to the level of noise present in the image, and it locally adapts to the orientation of the structures within the image. Fig. 5 shows that the proposed algorithm is robust with respect to the total diffusion time that is applied during the processing. We observe that the estimated standard deviation of the noise decreases with the iterations and gets to values lower than 1, while the Mean Square Error is strictly decreasing. A total diffusion time of 2 seems to be sufficient to reach almost convergence of the diffusion process.

B. Real Datasets

To further verify the performance of our filtering method, experiments have been carried out on two real datasets.

The first one is a T2 3-D MRI volume, scanned in a 1.5 Tesla GE Echospeed system.[1] The volume is filtered using the ORNRAD filter. Results are on Fig. 7. We observe a good reduction of the noise, a preservation of the detailed structures and a better definition of the interface between different tissues.

The second dataset is a 3-D SPoiled Gradient-Recalled (SPGR) MR data set of dimension $256 \times 256 \times 124$ and spatial resolution 0.9375 mm $\times$ 0.9375 mm $\times$ 1.5 mm. The original and filtered datasets are depicted in Fig. 8, on both three orthogonal slices of the whole volume: coronal, sagittal and axial respectively at left, middle and top positions, and a selected region-of-interest of a sagittal slice. The filter was run with the following parameters: structure tensor Gaussian kernel of standard deviations $\sigma_1 = 0.7$ mm and $\sigma_2 = 1.4$ mm, local statistics computed on a $3\times3\times3$ neighborhood, time-step $dt = 1/6$, and total diffusion time of $T = 2$. The estimated noise standard deviation on a selected region-of-interest is reduced from 5 to 0.8. When visually comparing the original and the filtered images on the region-of-interest, Fig. 8(c) and (d), we can appreciate the contrast enhancing at the interface between

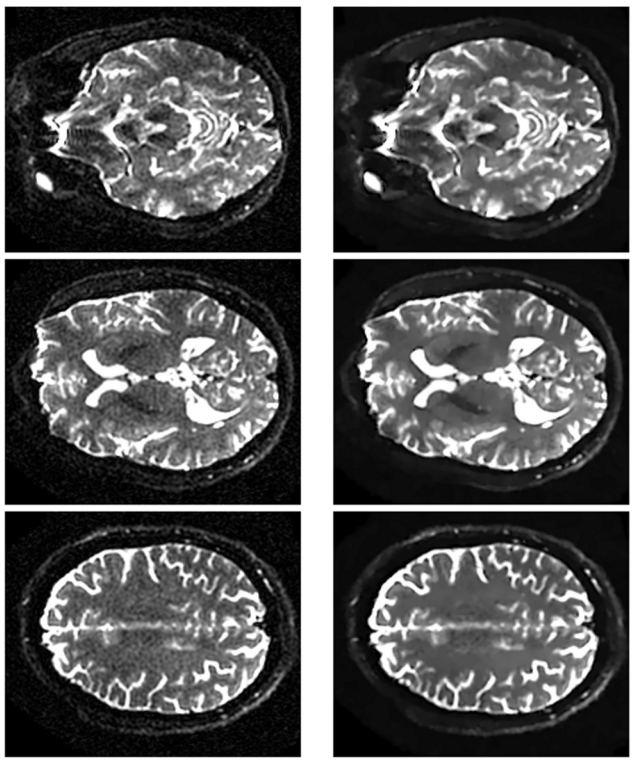

Fig. 7. Results on a 3-D T2-MR dataset, on three different axial slices. Left: original image; right: image filtered with the proposed filter.

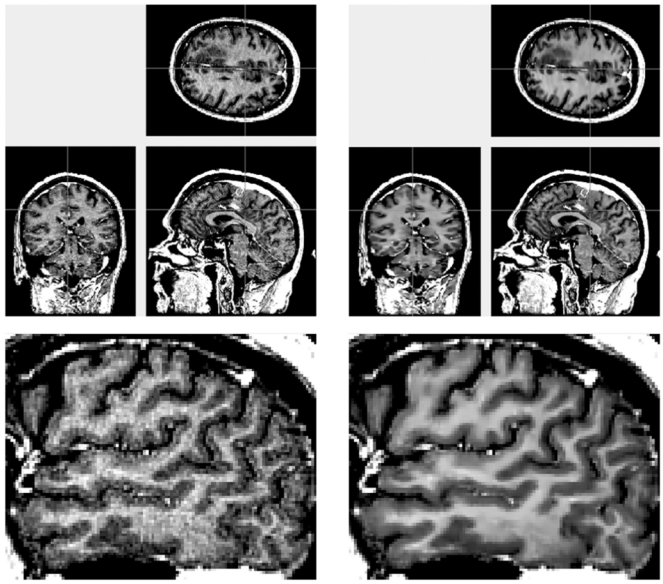

Fig. 8. Results on a 3-D SPGR dataset. Left: original dataset, right: image filtered with the proposed ORNRAD filter, top: three orthogonal slices; bottom: zoom on the sagittal slice.

[1]The scanning Sequence used maximum gradient amplitudes of 40 mT/M, six images with 4 high (750 s/mm^2), and two with low (5 s/mm^2) diffusion weighting. The rectangular field of view is 220 $\times$ 165 mm, the scan matrix 128 $\times$ 96 (256 $\times$ 192 image matrix), with 4 mm slice thickness and 1 mm interslice distance. Receiver bandwidth $\pm$6 kHz. TE (echo time) 70 ms; TR (repetition time) 80 ms (effective TR 2500 ms). Scan time 60 s/slice.

gray and white matter tissues and the noise removal within each tissue area. Small thin structures like vessels, appearing as white dots, are also well preserved by the algorithm.

V. Conclusion

A new filter designed to reduce Rician noise in Magnetic Resonance Images has been proposed. This filter is adapted from the Speckle Reducing Anisotropic Diffusion filter recently proposed in the context of Ultrasound images. It combines a Linear Minimum Mean Square Error filter applied to Rician noise distribution and the Perona and Malik's anisotropic diffusion filter. We have further extended the partial differential equation to use a diffusion matrix instead of a scalar, allowing a better reduction of the noise at contour locations. This new extension, based on the eigenvectors of the structure tensor, combines a smoothing of isotropic, planar and linear local structures, where each smoothing is weighted according to the corresponding LMMSE filter.

The new filter does not require the user to choose a contrast parameter for the edges of the structures like the standard Perona and Malik's filter, but relies instead on the local statistics of the image: local mean and local variance, and on an estimated standard deviation of the noise for the underlying noise model. Therefore, it needs a good estimation of the noise level, and a correct hypothesis about its statistical distribution. Based on previous publication, we choose to estimate the noise standard deviation as the mode of the local standard deviations on a subvolume of the image that does not contains background voxels.

A semi-implicit numerical scheme is presented to solve the PDE, based on the Jacobi scheme that allows easy multithreaded implementation. As a result of using a LMMSE approach and estimating the noise level at each iteration, the proposed filter is very robust to the total diffusion time and converges fast. Moreover, it requires very few parameter tuning since we used the same set of parameters for all our experiments, except for the standard deviation of the Gaussian kernel used to compute the structure tensor which needs to adapt to the voxels dimensions.

Experiments have been carried out on simulated and real data sets. Quantitative results using three different quality measures show a better behavior of the proposed scheme when compared to other state-of-the-art filters for different noise levels. According to the QILV, the scalar version of the filter gives slightly better results in edge preservation, while the matrix version shows a better performance in noise reduction.

A free implementation of the filter is available as part of the AMILab software.[2]

Future work includes extending this technique to multichannel data, and applying it in the context of Diffusion Tensor MRI. Another interesting extension to this work would be to evaluate the improvement of using our filter as a preprocessing step to other image processing techniques like segmentation and registration.

References

[1] R. Henkelman, "Measurement of signal intensities in the presence of noise in MR images," *Med. Phys.*, vol. 12, no. 2, pp. 232–233, 1985.

[2] G. McGibney and M. Smith, "Unbiased signal-to-noise ratio measure for magnetic resonance images," *Med. Phys.*, vol. 20, no. 4, pp. 1077–1078, 1993.

[3] J. Sijbers, A. J. den Dekker, P. Scheunders, and D. Van Dyck, "Maximum-likelihood estimation of Rician distribution parameters," *IEEE Trans. Med. Imag.*, vol. 17, no. 3, pp. 357–361, Jun. 1998.

[4] J. Sijbers and A. J. den Dekker, "Maximum likelihood estimation of signal amplitude and noise variance form MR data," *Magn. Res. Imag.*, vol. 51, pp. 586–594, 2004.

[5] M. D. DeVore, A. D. Lanterman, and J. A. O'Sullivan, "ATR performance of a Rician model for SAR images," in *Proc. SPIE*, Orlando, FL, Apr. 2000, pp. 34–37.

[6] R. Nowak, "Wavelet-based Rician noise removal for Magnetic Resonance Imaging," *IEEE Trans. Image Proccess.*, vol. 8, no. 10, pp. 1408–1419, Oct. 1999.

[7] A. Pižurica, W. Philips, I. Lemahieu, and M. Acheroy, "A versatile wavelet domain noise filtration technique for medical imaging," *IEEE Trans. Med. Imag.*, vol. 22, no. 3, pp. 323–331, Mar. 2003.

[8] T. McGraw, B. C. Vemuri, Y. Chen, M. Rao, and T. Mareci, "DT-MRI denoising and neuronal fiber tracking," *Med. Imag. Anal.*, vol. 8, pp. 95–111, 2004.

[9] G. Gerig, O. Kübler, R. Kikinis, and F. Jolesz, "Nonlinear anisotropic filtering of MRI data," *IEEE Trans. Med. Imag.*, vol. 11, no. 2, pp. 221–232, Jun. 1992.

[10] Y. Zhang, M. Brady, and S. Smith, "Segmentation of brain MR images through a hidden Markov random field model and the expectation-maximization algorithm," *IEEE Trans. Med. Imag.*, vol. 20, no. 1, pp. 45–57, Jan. 2001.

[11] S. Awate and R. Whitaker, "Nonparametric neighborhood statistics for MRI denoising," in *Information Processing in Medical Imaging*, ser. Lecture Notes in Computer Science. New York: Springer, Jul. 2005, vol. 3565, pp. 677–688.

[12] P. Coupé, P. Yger, S. Prima, P. Hellier, C. Kervrann, and C. Barillot, "An optimized blockwise non local means denoising filter for 3D magnetic resonance images," *IEEE Trans. Med. Imag.*, vol. 27, no. 4, pp. 425–441, Apr. 2008.

[13] J. V. Manjón, J. Carbonell-Caballero, J. J. Lull, G. García-Martí, L. Martí-Bonmatí, and M. Robles, "MRI denoising using non-local means," *Med. Image Anal.*, vol. 12, pp. 514–523, 2008.

[14] N. Wiest-Daesslé, S. Prima, P. Coupé, S. Morrissey, and C. Barillot, "Rician noise removal by non-local means filtering for low signal-to-noise ratio MRI: Applications to DT-MRI," in *Medical Image Computing and Computer-Assisted Intervention*, ser. Lecture Notes in Computer Science. New York: Springer-Verlag, 2008, vol. 5242, pp. 171–179.

[15] S. Aja-Fernández and K. Krissian, "An unbiased non-local means scheme for DWI filtering," in *Proc. Workshop on Computational Diffusion MRI, MICCAI*, 2008, pp. 277–284.

[16] S. Basu, T. Fletcher, and R. Whitaker, "Rician noise removal in diffusion tensor MRI," in *Proc. MICCAI*, 2006, vol. 1, pp. 117–125.

[17] C. G. Koay and P. J. Basser, "Analytically exact correction scheme for signal extraction from noisy magnitude MR signals," *J. Magn. Res.*, vol. 179, pp. 317–322, 2006.

[18] M. Martin-Fernandez, C. Aberola-Lopez, J. Ruiz-Alzola, and C.-F. Westin, "Sequential anisotropic Wiener filtering applied to 3D MRI data," *Magn. Reson. Imag.*, vol. 25, pp. 278–292, 2007.

[19] S. Aja-Fernández, C. Alberola-López, and C.-F. Westin, "Noise and signal estimation in magnitude MRI and Rician distributed images: A LMMSE approach," *IEEE Trans. Image Proccess.*, vol. 17, no. 8, pp. 1383–1398, Aug. 2008.

[20] S. Aja-Fernández, M. Niethammer, M. Kubicki, M. E. Shenton, and C.-F. Westin, "Restoration of DWI data using a rician LMMSE estimator," *IEEE Trans. Med. Imag.*, vol. 27, no. 10, pp. 1389–1403, Oct. 2008.

[21] A. Tristán-Vega and S. Aja-Fernández, "Joint LMMSE estimation of DWI data for DTI processing," in *Medical Image Computing and Computer-Assisted Intervention*, ser. Lecture Notes in Computer Science. New York: Springer-Verlag, Sep. 2008, vol. 5242, pp. 27–34.

[22] Y. Yu and S. Acton, "Speckle reducing anisotropic diffusion," *IEEE Trans. Image Proccess.*, vol. 11, no. 11, pp. 1260–1270, Nov. 2002.

[23] P. Perona and J. Malik, "Scale-space and edge detection using anisotropic diffusion," *IEEE Trans. Pattern Anal. Mach. Intell.*, vol. 12, no. 7, pp. 629–639, Jul. 1990.

[24] J. Lee, "Digital image enhancement and noise filtering using local statistics," *IEEE Trans. Pattern Anal. Mach. Intell.*, vol. 2, no. 2, pp. 165–168, Mar. 1980.

[2] http://amilab.sourceforge.net.

[25] S. Aja-Fernández and C. Alberola-López, "On the estimation of the coefficient of variation for anisotropic diffusion speckle filtering," *IEEE Trans. Image Proccess.*, vol. 15, no. 9, pp. 2694–2701, Sep. 2006.
[26] D. T. Kuan, A. A. Sawchuk, T. C. Strand, and C. P., "Adaptive noise smoothing filter with signal-dependent noise," *IEEE Trans. Pattern Anal. Mach. Intell.*, vol. 7, no. 2, pp. 165–177, Mar. 1985.
[27] K. Krissian, C. Westin, R. Kikinis, and K. Vosburgh, "Oriented speckle reducing anisotropic diffusion," *IEEE Trans. Image Proccess.*, vol. 16, no. 5, pp. 1412–1424, May 2007.
[28] D. Drumheller, "General expressions for Rician density and distribution functions," *IEEE Trans. Aerosp. Electron. Syst.*, vol. 29, no. 2, pp. 580–588, Apr. 1993.
[29] M. Brummer, R. Mersereau, R. Eisner, and R. Lewine, "Automatic detection of brain contours in MRI data sets," *IEEE Trans. Med. Imag.*, vol. 12, no. 2, pp. 153–166, Feb. 1993.
[30] J. Sijbers, D. Poot, A. J. den Dekker, and W. Pintjens, "Automatic estimation of the noise variance from the histogram of a magnetic resonance image," *Phys. Med. Biol.*, vol. 52, pp. 1335–1348, 2007.
[31] J. Sijbers, A. J. den Dekker, J. Van Audekerke, M. Verhoye, and D. Van Dyck, "Estimation of the noise in magnitude MR images," *Magn. Reson. Imag.*, vol. 16, no. 1, pp. 87–90, 1998.
[32] K. Krissian, "Flux-based anisotropic diffusion applied to enhancement of 3D angiogram," *IEEE Trans. Med. Imag.*, vol. 21, no. 11, pp. 1440–1442, Nov. 2002.
[33] M. Rodriguez-Florido, K. Krissian, J. Ruiz-Alzola, and C.-F. Westin, "Comparison of two restoration techniques in the context of 3D medical imaging," in *MICCAI01 Utrecht, The Netherlands*, ser. Lecture Notes in Computer Science. New York: Springer, 2001, vol. 2208, pp. 1031–1039.
[34] G. Farnebäck, "Polynomial Expansion for Orientation and Motion Estimation," Ph.D. dissertation, Linköping Univ., Linköping, Sweden, 2002, ISBN 91-7373-475-6, SE-581 83 Linköping, Sweden, dissertation No 790.
[35] K. Krissian and G. Farnebäck, "Technique for Enhancement of 3D angiograms and their applications," in *Medical Imaging Systems Technology: Methods in Cardiovascular and Brain Systems*. Singapore: World Scientific, 2005, pp. 359–396.
[36] J. Weickert, *Anisotropic Diffusion in Image Processing*. Stuttgart, Germamy: Teubner-Verlag, 1998.
[37] J. Bigün, G. H. Granlund, and J. Wiklund, "Multidimensional orientation: Texture analysis and optical flow," *IEEE Trans. Pattern Anal. Mach. Intell.*, vol. PAMI-13, no. 8, Aug. 1991.
[38] N. Otsu, "A threshold selection method from gray-scale histogram," *IEEE Trans. Syst., Man, Cybern.*, vol. 9, no. 1, pp. 62–66, Jan. 1979.
[39] T. Kurita, N. Otsu, and N. Abdelmalek, "Maximum likelihood thresholding based on population mixture models," *Pattern Recognit.*, vol. 25, no. 10, pp. 1231–1240, Oct. 1992.
[40] S. Aja-Fernández, G. Vegas-Sánchez-Ferrero, M. Martín-Fernández, and C. Alberola-López, "Automatic noise estimation in images using local statistics. Additive and multiplicative cases," *Image Vis. Comput.*, in press.
[41] D. Collins, A. Zijdenbos, V. Killokian, J. Sled, N. Kabani, C. Holmes, and A. Evans, "Design and construction of a realistic digital brain phantom," *IEEE Trans. Med. Imag.*, vol. 17, no. 3, pp. 463–468, Jun. 1998.
[42] A. Buades, B. Coll, and J. Morel, "A review of image denoising algorithms, with a new one," *Multiscale Model. Simul.*, vol. 4, no. 2, pp. 490–530, 2005.
[43] Z. Wang, A. C. Bovik, H. R. Sheikh, and E. P. Simoncelli, "Image quality assessment: From error visibility to structural similarity," *IEEE Trans. Image Proccess.*, vol. 13, no. 4, pp. 600–612, Apr. 2004.
[44] S. Aja-Fernández, R. San-José-Estépar, C. Alberola-López, and C.-F. Westin, "Image quality assesment based on local variance," in *Proc. 28th IEEE EMBC*, New York, Sep. 2006, pp. 4815–4818.

Karl Krissian received the M.S. degree in computer science and artificial intelligence from the University of Paris XI and the Ecole Normale Supérieure de Cachan in 1996 and the Ph.D. degree in computer vision from the University of Nice-Sophia Antipolis and the INRIA in 2000.

He worked at the University of Las Palmas from February 2000 to August 2001, at the Brigham and Women's Hospital and Harvard Medical School in Boston, MA, from September 2001 to November 2005, and at the University of Las Palmas since December 2005, where he is with the program Ramón y Cajal. His current research topics are denoising, segmentation, and registration of three-dimensional data sets for medical applications and, in particular, ultrasound images and vascular structures.

Santiago Aja-Fernández received the Ingeniero de Telecomunicación and the Ph.D. degrees from the University of Valladolid, Spain, in 1999 and 2003, respectively.

He is an Assistant Professor with the E.T.S.I. Telecomunicación, University of Valladolid, where he is also with the Laboratory of Image Processing (LPI). His research interests include medical image analysis and processing.

Dr. Aja-Fernández was awarded with a Fulbright Scholarship for a one-year stay as a Research Fellow with the LMI, Brigham and Women's Hospital.